



The effect of crab burrows on soil-water dynamics in mangroves

Marie Arnaud^{1,2,3} | Andy J. Baird² | Paul J. Morris² | Adam Taylor⁴ |
 Thuong Huyen Dang^{5,6} | Hanh Tran Hong⁵ | Thoai Dinh Quang⁵ |
 Tai Tue Nguyen⁷ | Pierre Polsenaere¹

¹IFREMER, Littoral, Laboratoire Environnement et Ressources des Pertuis Charentais (LER-PC), La Tremblade, France

²School of Geography, University of Leeds, Leeds, UK

³School of Geography, Earth and Environmental Sciences, University of Birmingham, Birmingham, UK

⁴Groundwater Modelling Solutions Ltd, Shrewsbury, UK

⁵Faculty of Geology and Petroleum Engineering, University of Technology, Vietnam National University Ho Chi Minh City (VNU-HCM), Ho Chi Minh City, Vietnam

⁶Institute for Circular Economy Development, Vietnam National University Ho Chi Minh City (VNU-HCM), Ho Chi Minh City, Vietnam

⁷Faculty of Geology, VNU-University of Science, Hanoi, Vietnam

Correspondence

Marie Arnaud, Laboratoire Environnement et Ressources des Pertuis Charentais (LER-PC), IFREMER, La Tremblade BP133, France.
 Email: m.arnaud@gmail.com

Funding information

University of Leeds

Abstract

Many mangrove ecosystem services, such as carbon sequestration, are closely linked to mangrove soil water content, which in turn is thought to depend on animal burrow density and the properties of the sediment in which the burrows are constructed. We measured the water content in the sediment matrix between crab burrows across 26 plots in a typical, fine-grained (clay), mangrove soil in the Mekong Delta, Vietnam. We found that the water content of the sediment matrix remained more or less constant throughout the tidal cycle, and was independent of burrow density. Our results suggest that there is little exchange of water between the burrows and the associated sediment matrix and that burrows act as an independent pipe network transporting water through the mangrove soil. To check and extend our findings, we used a numerical groundwater model to simulate an idealized burrow in a range of sediment types. The model results confirmed that fine-grained mangrove sediments do not drain readily into adjacent animal burrows because of their very low permeability. Our results have important implications for understanding and forecasting mangrove carbon dynamics with sea level rise.

KEYWORDS

burrow, drainage, groundwater, mangrove soil, sediment matrix, soil water content

1 | INTRODUCTION

The degree to which mangrove soils drain during the tidal cycle is thought to be an important control on their carbon and nutrient cycles (Wolanski et al., 1992; Xiong et al., 2018). If mangrove sediments remain saturated, or close to saturated, throughout the tidal cycle, they will rarely experience oxic conditions, leading to slow mineralisation of organic matter. Mangroves are one of the most carbon dense ecosystems in the world (Donato et al., 2011), and

slow mineralisation of soil organic matter in permanently-saturated soils would promote their carbon capture and storage. However, it has also been suggested that the export of large quantities of organic matter, inorganic carbon and nutrients from mangroves to coastal waters must be due to large quantities of groundwater discharging from mangrove soils during the tidal cycle (Chen et al., 2021; Dittmar et al., 2006; Lee, 1995; Maher et al., 2013; Ridd, 1996; Santos et al., 2019; Stieglitz et al., 2000; Taillardat et al., 2018).

This is an open access article under the terms of the Creative Commons Attribution-NonCommercial-NoDerivs License, which permits use and distribution in any medium, provided the original work is properly cited, the use is non-commercial and no modifications or adaptations are made.

© 2022 The Authors. *Hydrological Processes* published by John Wiley & Sons Ltd.

Mangrove soils are characterized by a sediment matrix in which numerous animal burrows are often found. The drainage of a mangrove soil will be influenced by the hydraulic conductivity of the matrix—which in turn is related to sediment grain size—and by the density and connectivity of animal burrows (Susilo & Ridd, 2005). In addition, position within the tidal prism and the slope of the soil surface will control the overall hydraulic gradient, with more steeply-sloping mangrove soils expected to drain more readily than those with gentle slopes (Mazda et al., 2007; Mazda & Ikeda, 2006).

Several studies have investigated the influence of animal burrows on water flow in mangrove soils. Susilo and Ridd (2005) reported that crab burrows can increase the bulk hydraulic conductivity of mangrove soils by up to a factor of 10 but did not measure how the water content of the sediment matrix varied over the tidal cycle or how it was affected by burrow density (see below). Flushing of burrows may occur during tidal cycles, and is caused by pressure differences between burrow entrances and exits, due to their different positions on the sloping soil surface (Ridd, 1996; Stieglitz et al., 2000). Large-scale (forest-scale) studies using radioisotope tracer techniques have estimated that a large amount of water ($16.3 \pm 5.1 \text{ cm d}^{-1}$ on average; Tait et al., 2016) is exported from mangrove soils to adjacent tidal creeks (Stieglitz et al., 2013; Taillardat et al., 2018; Tait et al., 2016). This water seems to be highly enriched with dissolved inorganic carbon (DIC) (Taillardat et al., 2018), and represents one of the largest losses of mangrove carbon. Maher et al. (2017) found that DIC at one site was a century old and hypothesised this old DIC to be the product of aerobic mineralisation of sediments in the walls of crab burrows. However, this hypothesis has not yet been tested in the field.

It has been demonstrated that animal burrows increase the surface area of soil exposed to air (Kristensen et al., 2008). However, whether burrows cause the mangrove sediment matrix between burrows to drain more readily is still unclear (Susilo & Ridd, 2005). Both the sediment matrix and animal burrows can be expected to become largely water-filled as the tide rises. As the tide ebbs, burrows that have multiple openings may drain readily (Ridd, 1996; Stieglitz et al., 2000). Then, large hydraulic gradients may develop between the sediment matrix and the dewatering burrows, with water seeping from the former into the latter if the hydraulic conductivity of the sediment matrix permits it. If sufficient seepage occurs, the sediment

matrix will aerate, leading to higher rates of carbon mineralisation, and an increase in the inorganic carbon flux from the mangrove soil as has been observed in salt marshes (Xiao et al., 2021). However, low hydraulic conductivity in fine-grained mangrove sediments may prevent the matrix from draining despite the dewatering of burrows, leaving the majority of the soil profile largely hydrologically disconnected from coastal seas.

The filling and draining of both the burrows and sediment matrix during each tidal cycle corresponds with the sponge model of Alongi (2014) (Figure 1). In contrast, other authors (e.g., Tait et al., 2016) have suggested that most water flow in mangrove soils is restricted to the animal burrows, and that the sediment matrix does not drain. Better understanding of the hydrological dynamics of mangrove soils is important, because if the sediment matrix is mostly hydrologically inert and independent from the burrows, anoxic conditions will prevail in this part of the soil, reducing overall rates of soil organic matter decay. Furthermore, climate change might modify those processes. Sea level rise has been shown to have the potential to modify the sediment grain size composition (Sanders et al., 2012), which might in turn alter the associated soil-water dynamics.

To test whether both burrows and the sediment matrix drain during the tidal cycle, we measured in-situ the water content of the mangrove sediment matrix along a gradient of animal burrow densities and relative surface areas of burrow openings. Our study site in the Mekong Delta of Vietnam has a fine-grained (clayey) matrix typical of many mangroves (see Methods) (Figure 2). We also used a simulation model of groundwater flow between the sediment matrix and an idealized crab burrow to assess the kinds of sediment grain-size distributions that might reasonably be expected to give rise to appreciable drainage from the matrix during a tidal cycle.

2 | MATERIALS AND METHODS

2.1 | Study site

We undertook our field investigation at the Can Gio Biosphere Reserve (CGBR) in the Mekong Delta in the south of Vietnam (Figure 2). The site in CGBR is typical of many Southeast Asian mangroves, insofar

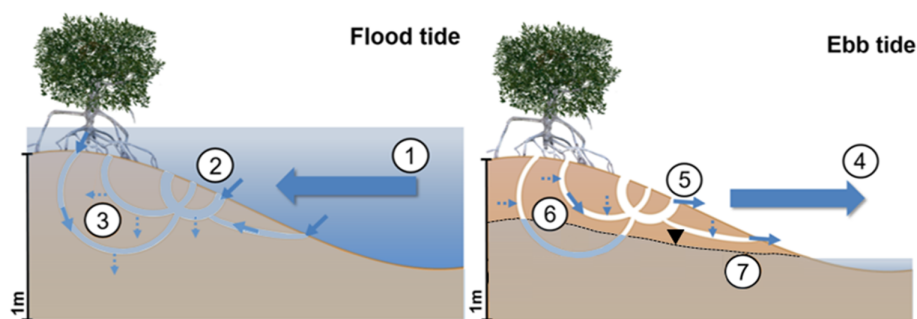
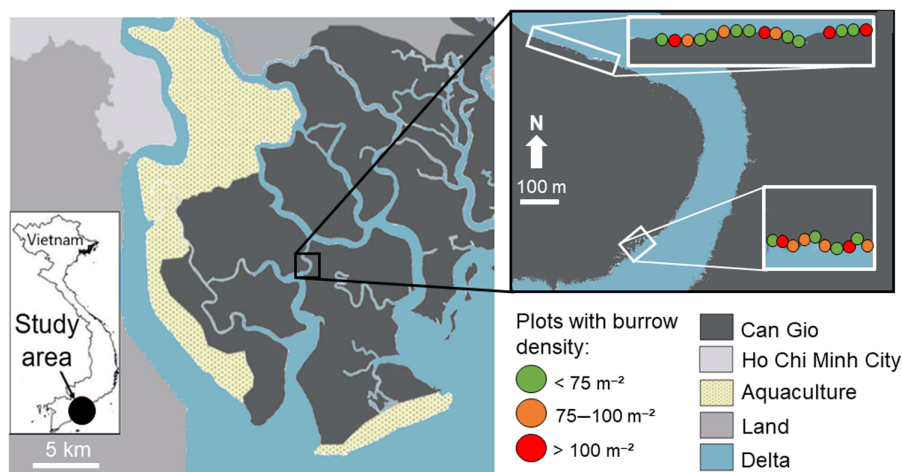


FIGURE 1 Conceptual hydrological model of mangrove soils based on the sponge model of Alongi (2014). Water from the incoming tide (1) enters the burrows (2), flows through the burrow network and infiltrates into the sediment matrix (3). At ebb tide, there is an outwelling of solute-enriched groundwater (4) resulting from the drainage of the burrows (5) and the sediment matrix (6). This drainage causes the water table in the soil, including the sediment matrix, to fall (7). In Alongi's (2014) original model the water table at low tide is shown as a flat line coincident with the tide level, which is not plausible even in more permeable sandy sediments (e.g., Baird et al., 1998)

FIGURE 2 Location of the study area and distribution of the monitoring plots. Modified from Arnaud et al. (2021) and Taillardat et al. (2018)



as: (i) it is a dense carbon store ($910.7 \pm 32.2 \text{ t C ha}^{-1}$ [Dung et al., 2016]); (ii) it is dominated by trees of the *Rhizophora* genus (Arnaud et al., 2021; Donato et al., 2011); (iii) the sediment matrix is mostly composed of clay-sized grains (70% of sediment by weight: Arnaud et al., 2020), which is typical of deltaic or riverine mangroves (Woodroffe, 1992); and (iv) it has an average groundwater outwelling discharge of between 3.1 and 7.1 cm day^{-1} , which is within the range previously reported in mangroves more broadly (Taillardat et al., 2018; Tait et al., 2016). The tidal regime is irregular and semi-diurnal, with a maximum amplitude of $3.3\text{--}4.1 \text{ m}$ in October and November (Thi Hoa Binh et al., 2008; Van Loon et al., 2016). The macrofauna associated with burrowing activities found in this site appear to be dominated by sesamid (family Grapsidae) and fiddler crabs (family Ocypodidae; genus *Uca*) (Diele et al., 2013). Burrows of fiddler crab are J- or L-shaped in vertical section and between 20 and 40 cm deep (Kristensen, 2008). In contrast, burrows of sesamid crabs range from simple, straight burrows with few branches to complex, labyrinthine structures with multiple openings over depths between 55 and 110 cm (Kristensen, 2008). CGBR has a low-lying topography with elevation ranging from 0.5 to 1.5 m above mean sea level. Our measurement plots were located in the mudflat (mid-intertidal) zone.

2.2 | Water content measurements and observations

We took more than 1400 soil water-content measurements across $26 \text{ m} \times 1 \text{ m}$ plots located in the mid-inter-tidal area of CGBR. We also recorded video footage of burrows being filled during a flood tide (Supporting Information 1). To investigate how burrows affect sediment drainage, the plots were chosen to cover a range of densities and surface areas of burrow openings (Figure 3). Thus, the plots were not chosen randomly. In each plot we established between 15 and 20 fixed points in the sediment matrix from which we took repeated measurements of soil volumetric water content (VWC) during that part of the tidal cycle when the plot was not covered in water and, for safety reasons, during hours of daylight. The measurements were

taken over 5 days of medium to high tidal amplitude in October and December 2018. To limit confounding effects, we chose plots with similar elevations above the mean sea level, and which were mostly free of dense belowground roots. We took all the in-situ measurements from floating platforms to avoid disturbance to the measurement plots (Supporting Information 1). When grounded, these platforms exerted low pressures on the soil surface and had no obvious effects on the water content of the sediment matrix between the burrow openings. We measured VWC of the sediment matrix using a ThetaProbe (DeltaT Devices; Cambridge, UK).

We took measurements at approximately one-hour intervals for up to 4.5 h . The ThetaProbe measures VWC in a cylinder of sediment 3 cm in diameter and 6 cm in length (Gaskin & Miller, 1996). The VWC measured was therefore in the top soil, which is the part of the soil most prone to drainage. We calibrated the ThetaProbe with sediments collected from the field site. From saturation, we dried the calibration sediments in an oven set at 30°C . During the drying, we took regular ThetaProbe readings, and reweighed the sediments each time to calculate changes in water content. ThetaProbes have a typical accuracy of $\pm 1\%$ for soil-specific calibrations (manufacturer's information). Our calibration over the moisture range encountered in the field had an r^2 of 0.94 .

2.3 | Determination of areal coverage and density of burrow openings

We measured the number of burrow openings per unit area, and their areal coverage, from digital photographs of the plots (such as that shown in Figure 3). In total, we measured more than 2000 burrow openings. We corrected each picture for image distortion with the GNU Image Manipulation Program (GIMP) (<https://www.gimp.org/>) and then extracted the area and the number of burrow openings in each image using ImageJ (Rueden et al., 2017). The area and number of the burrows were obtained by converting each image into an 8-bit greyscale image. The threshold tool was then used to increase the contrast and separate the burrows (black pixels) from the soil matrix

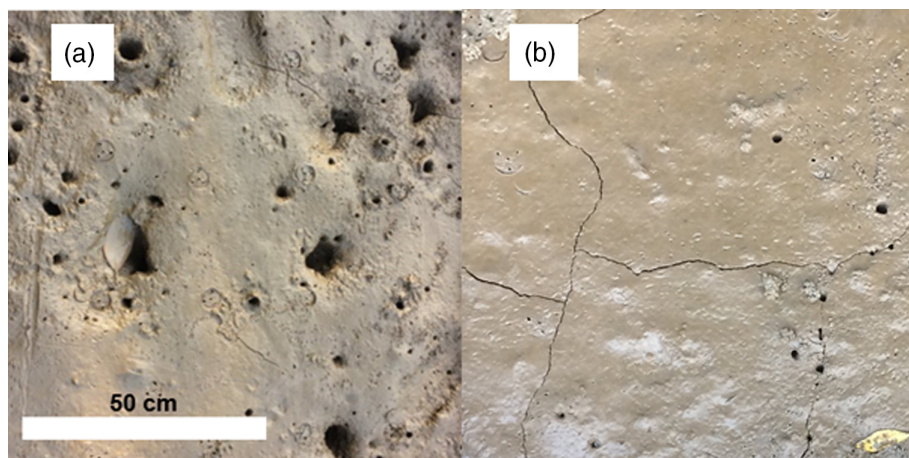


FIGURE 3 Examples of burrow openings in plots with (a) high (>100 burrows m^{-2}) and (b) low (<75 burrows m^{-2}) burrow density

(white pixels) for each image. Finally, we used the 'region of interest (ROI) manager tool' with the function 'measure' to obtain the area of each burrow opening, as well as their number for each image. We measured only burrow openings with a minimum area of 0.50 cm^2 (~ 8 mm diameter), because smaller burrow openings could not be differentiated in ImageJ from crab defecation pellet shadows.

2.4 | Modelling of water flow into an idealized burrow

To check our interpretation of our field data and to extend our results to sediments with different grain sizes, we used a 3-D groundwater model to simulate flow into a single vertical burrow that is 50 cm long (Figure 4), has a diameter of 6 cm, and in which the water level is fixed at a depth of 5 cm from the burrow base (45 cm depth), as shown in Figure 4. Our approach is similar to that used by Xin et al. (2009) and Xiao et al. (2019), who simulated the effect of crab burrows in layered sediments in salt marshes. Both Xin et al. (2009) and Xiao et al. (2019) represented multiple crab burrows as simple vertical columns of high-permeability sediment, and both saturated and unsaturated flow were simulated. We simulated saturated flow only, accounting for water-table rise and fall using the specific yield of the sediment (see below). As with Xin et al. (2009) and Xiao et al. (2019), we assumed Darcy's law applied to the flow within the sediment. We represented the crab burrow in a more realistic way than Xin et al. (2009) and Xiao et al. (2019): it was treated as an air-filled void and a seepage face was allowed to develop on the wall of the burrow.

Our 3-D model accounts for radial flow to the burrow, both in plan and with depth. We built the model using Modflow 6 (Supporting Information 2). In each model run, we assumed the sediment matrix had a single, uniform combination of hydraulic conductivity and specific yield, summarized in Table 1. We considered five combinations of hydraulic conductivity and specific yield to represent two types of clay and three types of silt (Table 1). In each case, we used the model to simulate 6 h of drainage, assuming an initial condition in which the sediment matrix beyond the burrow was saturated (the water table

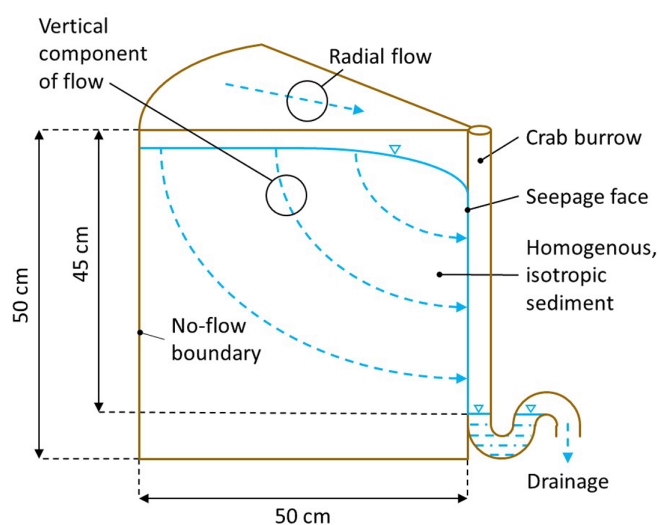


FIGURE 4 Geometry of the idealized crab burrow represented in the numerical model

was at the mangrove surface). Further details of the model are provided in Supporting Information 2.

3 | RESULTS AND DISCUSSION

3.1 | Water content of the sediment matrix is unaffected by the presence of crab burrows

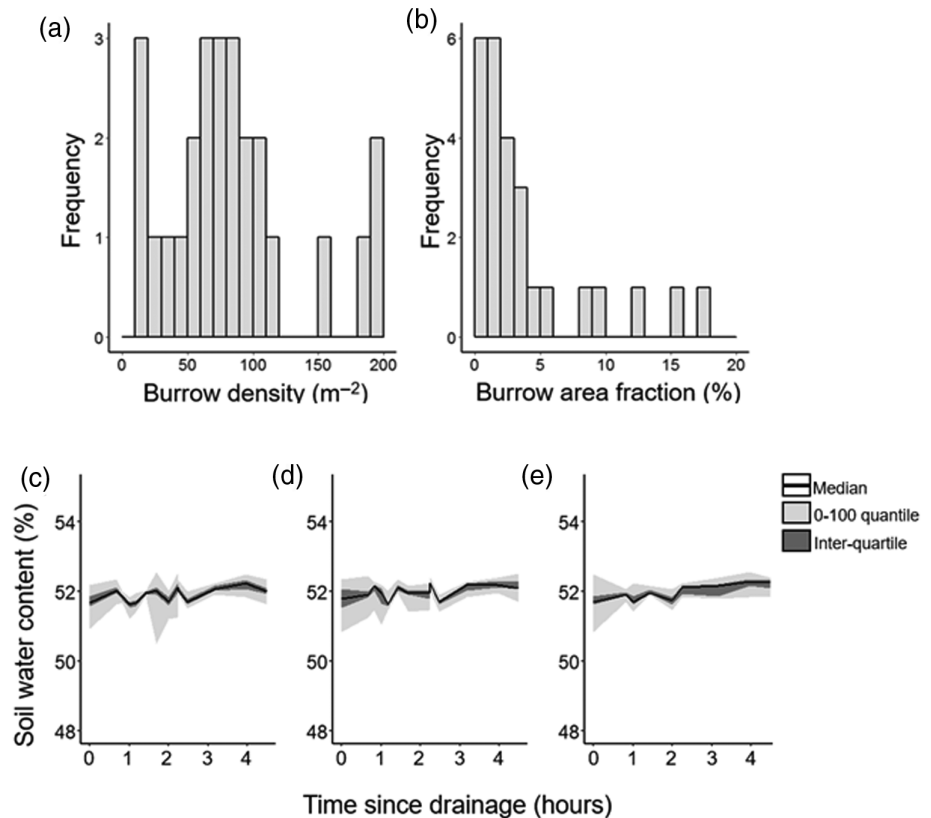
Our in-situ measurements showed that the water content of the sediment matrix remained at, or close to, saturation, with very little variation over time (Figure 5). The minimum VWC of the sediment matrix per plot was 51.5% and the maximum was 52.2%. There was no obvious difference between the plots, despite: i) the number of burrow openings per plot differing by more than an order of magnitude (min = 11, max = 198), and ii) the area of the burrow openings being more than two orders of magnitude greater in the plot that was most

TABLE 1 Hydraulic conductivity and specific yield values used in the numerical model simulations

	Fine clay ^{a,b}	Coarse clay ^{a,b}	Fine silt ^{a,b}	Medium silt	Coarse silt ^{a,b}
Hydraulic conductivity (m s^{-1})	1×10^{-11}	4.7×10^{-9}	1×10^{-9}	1×10^{-7}	2×10^{-5}
Specific yield (–)	0.03	0.03	0.08	0.08	0.08

Note: ^aDenotes values taken from table 3.2 and ^b from table 4.2, both in Domenico and Schwartz (1990). The hydraulic conductivity for the medium silt was set to be $100 \times$ greater than the value for the fine silt. Domenico and Schwartz (1990) do not define these particle size terms. However, one of the main sources of their information (Johnson, 1967) classifies sand as a particle size of 2–0.0625 mm, silt as 0.0625–0.004 mm, and clay as <0.004 mm. No information is provided in Domenico and Schwartz (1990) on the boundaries between ‘fine’, ‘medium’ and ‘coarse’.

FIGURE 5 Results from the field plots: (a) burrow opening density, (b) burrow opening area fraction. (c–e) show the median (black line) and the distribution of the data (0–100% quantile range in light grey; and inter-quartile range in dark grey) of the VWC of the sediment matrix in plots having a (c) low (<75 burrows m^{-2}), (d) medium (75–100 burrows m^{-2}) and high (e) (>100 burrows m^{-2}) density of burrows



heavily-burrowed compared to plots that were almost free of burrows (Figure 5).

As noted above, several studies have shown a large exchange of water between mangrove forests and adjacent water bodies, including previous work at our study site (Taillardat et al., 2018). Our VMC measurements suggest that such exchange must take place wholly in the animal burrows. Our burrow data can be used as a check on this finding. We measured a mean surface burrow area fraction of 4%, although this figure is based on a non-random sample (see Methods). If we assume that the unit volume of burrows is similar to this value, and that burrows extend to a depth of 50–100 cm, the total volume occupied by burrows is equivalent to a water depth of 2–4 cm. If we further assume that all of the burrow volume is flushed per tidal cycle, then two tidal cycles per day could flush 4–8 cm day^{-1} , a range very close to the 3.1–7.1 cm day^{-1} recorded elsewhere at Can Gio by Taillardat et al. (2018). Clearly, such an analysis is only very approximate, but it does suggest that drainage of the sediment matrix does not need to be invoked to explain existing groundwater flushing estimates.

We also observed the rapid filling and drainage of the crab burrows in our plots confirming that burrows must have two or more openings, as observed by Stieglitz et al. (2000). The video (Supporting Information 1) shows burrows filling from below as well as from above as the tide rises. Burrows filling rapidly from below can only be explained by water entering another opening in the same burrow at a lower location that is already flooded with tidal water. Furthermore, the fact that the burrows are empty at the beginning of the video shows that they drain during low tide.

Overall, our observations confirm that the mangrove soil comprises a system of large hydrologically-dynamic macropores, in which water flow occurs readily, set within a microporous matrix where the turnover of water is very slow. Figure 6 summarizes our results as a conceptual model. Similar dual-porosity systems occur in terrestrial soils (Armstrong & Arrowsmith, 1986; Beven & Germann, 1982). The sediment matrix seems to be best described by hydraulic principles based on Darcy's Law, and the macropores as a separate soil domain in which turbulent or non-Darcian flow may occur (Beven & Germann, 1982). The limited interaction between these two domains is

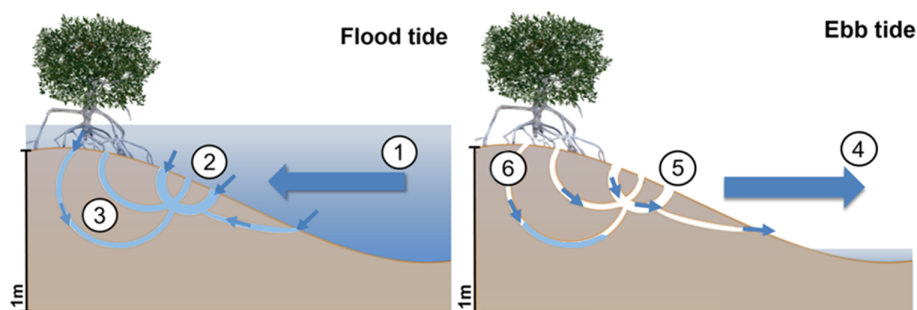


FIGURE 6 The dual-porosity and -permeability system of fine-grained mangrove soils, such as our study site. During flood tide (1), incoming water enters the burrows at their surface openings (2), flushing out air and filling them with water (3). During the ebb tide (4), water stored in the burrows, enriched in solutes derived from the burrow walls, drains (5). Although the burrows drain, the water table in the sediment matrix remains stable at or near the ground surface (6)

likely to result from the mangrove sediment having a very low hydraulic conductivity. We used the modelling work to check that this conclusion is plausible from a process-based perspective, and to explore the implications for mangroves across a range of sediment grain sizes.

3.2 | Modelling water exchanges between the sediment matrix and crab burrows

The numerical model results (Figure 7) confirm our interpretation of the field data and show that, in a crab burrow surrounded by a clay, there is likely to be little or no drainage between the sediment matrix and the burrow during a typical tidal cycle. The ranges of hydraulic conductivity values reported for clays and silts overlap (Figure 7). For the bottom end of the clay range (fine clay in Figure 7 and Table 1) and the bottom end of the silt range (fine silt), virtually no water flows between the sediment and the modelled burrow. For the high end of the clay range, which is higher than the lower end of the silt range, a small amount of sediment drainage occurs within 15 cm of the burrow. These results confirm that for the low hydraulic conductivities of most clays and fine silts, water does not drain into crab burrows during the tidal cycle. The simulation of the higher end of hydraulic conductivities, representing coarse silt, did show substantial drainage to the crab burrow, and is consistent, in part at least, with Alongi's (2014) model (Figure 1). As shown in Figure 7, even after only 1.5 h, more than half of the coarse silt within the vicinity of the burrow had drained, releasing water representing 8% of the total volume of the matrix. Clearly, our simulations are idealized and do not include real-world spatial complexity such as multiple burrows and burrow angles, which would prove numerically challenging or intractable. However, in combination with our field data, they suggest that water exchanges between fine-grained mangrove soils and adjacent open-water bodies are confined almost wholly to the burrow network. Since clay and fine silt are the dominant grain size fraction found in many mangrove sediments (Woodroffe, 1992), our findings can be expected to have wide applicability. For mangroves containing coarse silts and sands, Alongi's (2014) sponge model will be more appropriate. Our measurements and modelling are limited to sediments that were well sorted, in

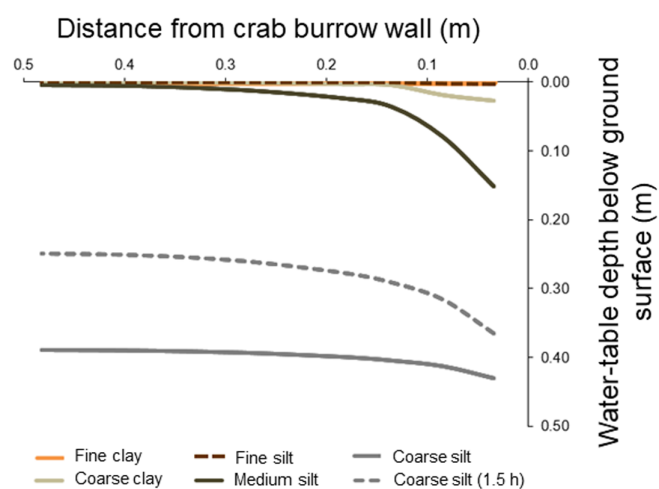


FIGURE 7 Results from the numerical model runs for the situation depicted in Figure 4. All water tables are for 6 h after the commencement of drainage, except the grey dashed line, which shows the position of the water table after 1.5 h

the case of poorly sorted sediments more studies will be necessary to establish the effects on drainage.

3.3 | Implication for biogeochemical processes

Our results have several implications for biogeochemical cycling in mangroves. The water table does not fluctuate substantially in the sediment matrix, meaning that the mangrove sediment matrix will be mostly anoxic, which likely aids mangrove carbon sequestration by decreasing mineralisation rates. Burrow walls, however, may act as hot-spots of carbon mineralisation and nutrient cycling, by increasing the total surface area of the sediment matrix exposed to the air during low water (Kristensen et al., 2012). Crabs ingest organic matter and redeposit it in the form of defecation pellets at the surface of the sediment matrix or inside burrows (Kristensen et al., 2012). This mineralised carbon is readily available for daily tidal export in fringe mangroves. The twice-daily tidal inundation that brings fast-flowing

water through the burrow pipe network transports this matter to adjacent ecosystems, and may also cause some erosion of the burrow wall surface (personal in-situ observations by the senior author), increasing the quantity of matter exported.

4 | CONCLUSIONS

We found that the upper layer of a mangrove sediment matrix does not drain during ebb tides and that near-surface water contents are unaffected by animal burrows. Our results confirm that animal burrows do not cause drainage of the sediment matrix in fine-grained mangrove soils, and rather act as an independent pipe network through which water enters and leaves according to the tidal cycle, leaving the majority of the sediment matrix hydrologically disconnected from the ocean. Our simulation modelling indicates that exchanges of water between the sediment matrix and burrows are only likely to be important in mangroves with sediment grain-size distributions towards the coarse end of those usually observed.

ACKNOWLEDGEMENTS

We thank: David Ashley and David Roe (University of Leeds) for instrumentation support; the Can Gio Management board for permission to use the sites and hosting us; Niah and Hung Tran Trong (Can Gio Biosphere Reserve) who helped install the floating platforms; and Kanami Koike and Nodoka Ori (Hokkaido University) for their support in the field. This research received financial support from a University Research Scholarship and an International Mobility Grant, both from the University of Leeds, UK.

DATA AVAILABILITY STATEMENT

The data that support the findings of this study are available in the supplementary material of this article (Supporting Information 3).

ORCID

Marie Arnaud <https://orcid.org/0000-0003-4001-6499>

Andy J. Baird <https://orcid.org/0000-0001-8198-3229>

Paul J. Morris <https://orcid.org/0000-0002-1145-1478>

Thuong Huyen Dang <https://orcid.org/0000-0002-7844-1573>

Tai Tue Nguyen <https://orcid.org/0000-0002-8434-2766>

Pierre Polsemaere <https://orcid.org/0000-0002-2454-485X>

REFERENCES

- Alongi, D. M. (2014). Carbon cycling and storage in mangrove forests. *Annual Review of Marine Science*, 6(January 2014), 195–219. <https://doi.org/10.1146/annurev-marine-010213-135020>
- Armstrong, A. C., & Arrowsmith, R. (1986). Field evidence for a bi-porous soil water regime in clay soils. *Agricultural Water Management*, 11(2), 117–125. [https://doi.org/10.1016/0378-3774\(86\)90024-7](https://doi.org/10.1016/0378-3774(86)90024-7)
- Arnaud, M., Baird, A. J., Morris, P. J., Dang, T. H., & Nguyen, T. T. (2020). Sensitivity of mangrove soil organic matter decay to warming and sea level change. *Global Change Biology*, 26(3), 1899–1907. <https://doi.org/10.1111/gcb.14931>
- Arnaud, M., Morris, P. J., Baird, A. J., Dang, H., & Nguyen, T. T. (2021). Fine root production in a chronosequence of mature reforested mangroves. *New Phytologist*, 232(4), 1591–1602. <https://doi.org/10.1111/nph.17480>
- Baird, A. J., Mason, T., & Horn, D. P. (1998). Validation of a Boussinesq model of beach ground water behaviour. *Marine Geology*, 148, 55–69.
- Beven, K., & Germann, P. (1982). Macropores and water flow in soils. *Water Resources Research*, 18(5), 1311–1325. <https://doi.org/10.1029/WR018i005p01311>
- Chen, X., Santos, I. R., Call, M., Reithmaier, G. M. S., Maher, D., Holloway, C., Wadnerkar, P. D., Gómez-Álvarez, P., Sanders, C. J., & Li, L. (2021). The mangrove CO₂ pump: Tidally driven pore-water exchange. *Limnology and Oceanography*, 66(4), 1563–1577. <https://doi.org/10.1002/lno.11704>
- Diele, K., Tran Ngoc, D. M., Geist, S. J., Meyer, F. W., Pham, Q. H., Saint-Paul, U., Tran, T., & Berger, U. (2013). Impact of typhoon disturbance on the diversity of key ecosystem engineers in a monoculture mangrove forest plantation, Can Gio Biosphere Reserve, Vietnam. *Global and Planetary Change*, 110, 236–248. <https://doi.org/10.1016/j.gloplacha.2012.09.003>
- Dittmar, T., Hertkorn, N., Kattner, G., & Lara, R. J. (2006). Mangroves, a major source of dissolved organic carbon to the oceans. *Global Biogeochemical Cycles*, 20(1). <https://doi.org/10.1029/2005GB002570>
- Domenico, P. A., & Schwartz, F. W. (1990). *Physical and chemical hydrogeology* (2nd ed.). Wiley.
- Donato, D. C., Kauffman, J. B., Murdiyarso, D., Kurnianto, S., Stidham, M., & Kanninen, M. (2011). Mangroves among the most carbon-rich forests in the tropics. *Nature Geoscience*, 4(5), 293–297. <https://doi.org/10.1038/ngeo1123>
- Dung, L. V., Tue, N. T., Nhuan, M. T., & Omori, K. (2016). Carbon storage in a restored mangrove forest in Can Gio Mangrove Forest Park, Mekong Delta, Vietnam. *Forest Ecology and Management*, 380, 31–40. <https://doi.org/10.1016/j.foreco.2016.08.032>
- Gaskin, G. J., & Miller, J. D. (1996). Measurement of soil water content using a simplified impedance measuring technique. *Journal of Agricultural Engineering Research*, 63(2), 153–159. <https://doi.org/10.1006/jaer.1996.0017>
- Johnson, A. I. (1967). Specific yield – Compilation of specific yields for various Materials. USGS water supply paper 1667-D, 74 pp.
- Kristensen, E. (2008). Mangrove crabs as ecosystem engineers; with emphasis on sediment processes. *Journal of Sea Research*, 59(1–2), 30–43. <https://doi.org/10.1016/j.seares.2007.05.004>
- Kristensen, E., Bouillon, S., Dittmar, T., & Marchand, C. (2008). Organic carbon dynamics in mangrove ecosystems: A review. *Aquatic Botany*, 89(2), 201–219. <https://doi.org/10.1016/j.aquabot.2007.12.005>
- Kristensen, E., Penha-Lopes, G., Delefosse, M., Valdemarsen, T., Quintana, C., & Banta, G. (2012). What is bioturbation? The need for a precise definition for fauna in aquatic sciences. *Marine Ecology Progress Series*, 446, 285–302. <https://doi.org/10.3354/meps09506>
- Lee, S. Y. (1995). Mangrove outwelling: A review. *Hydrobiologia*, 295(1–3), 203–212. <https://doi.org/10.1007/BF00029127>
- Maher, D. T., Santos, I. R., Golsby-Smith, L., Gleeson, J., & Eyre, B. D. (2013). Groundwater-derived dissolved inorganic and organic carbon exports from a mangrove tidal creek: The missing mangrove carbon sink? *Limnology and Oceanography*, 58(2), 475–488. <http://www.scopus.com/inward/record.url?eid=2-s2.0-84875363148&partnerID=tZ0tx3y1>
- Maher, D. T., Santos, I. R., Schulz, K. G., Call, M., Jacobsen, G. E., & Sanders, C. J. (2017). Blue carbon oxidation revealed by radiogenic and stable isotopes in a mangrove system. *Geophysical Research Letters*, 44(10), 4889–4896. <https://doi.org/10.1002/2017GL073753>
- Mazda, Y., & Ikeda, Y. (2006). Behavior of the groundwater in a riverine-type mangrove forest. *Wetlands Ecology and Management*, 14(6), 477–488. <https://doi.org/10.1007/s11273-006-9000-z>
- Mazda, Y., Wolanski, E., & Ridd, P. (2007). Outline of the physical processes within mangrove systems. The Role of Physical Processes in Mangrove Environments, 3–64.

- Ridd, P. V. (1996). Flow through animal burrows in mangrove creeks. *Estuarine, Coastal and Shelf Science*, 43(5), 617–625. <https://doi.org/10.1006/ecss.1996.0091>
- Rueden, C. T., Schindelin, J., Hiner, M. C., DeZonia, B. E., Walter, A. E., Arena, E. T., & Eliceiri, K. W. (2017). ImageJ2: ImageJ for the next generation of scientific image data. *BMC Bioinformatics*, 18(1), 529. <https://doi.org/10.1186/s12859-017-1934-z>
- Sanders, C. J., Smoak, J. M., Waters, M. N., Sanders, L. M., Brandini, N., & Patchineelam, S. R. (2012). Organic matter content and particle size modifications in mangrove sediments as responses to sea level rise. *Marine Environmental Research*, 77, 150–155. <https://doi.org/10.1016/j.marenvres.2012.02.004>
- Santos, I. R., Maher, D. T., Larkin, R., Webb, J. R., & Sanders, C. J. (2019). Carbon outwelling and outgassing vs. burial in an estuarine tidal creek surrounded by mangrove and saltmarsh wetlands. *Limnology and Oceanography*, 64(3), 996–1013. <https://doi.org/10.1002/lno.11090>
- Stieglitz, T., Ridd, P., & Müller, P. (2000). Passive irrigation and functional morphology of crustacean burrows in a tropical mangrove swamp. *Hydrobiologia*, 421(1–3), 69–76. <https://doi.org/10.1023/A:1003925502665>
- Stieglitz, T. C., Clark, J. F., & Hancock, G. J. (2013). The mangrove pump: The tidal flushing of animal burrows in a tropical mangrove forest determined from radionuclide budgets. *Geochimica et Cosmochimica Acta*, 102, 12–22. <https://doi.org/10.1016/j.gca.2012.10.033>
- Susilo, A., & Ridd, P. V. (2005). The bulk hydraulic conductivity of mangrove soil perforated with animal burrows. *Wetlands Ecology and Management*, 13(2), 123–133. <https://doi.org/10.1007/s11273-004-8324-9>
- Taillardat, P., Willemsen, P., Marchand, C., Friess, D. A., Widory, D., Baudron, P., Truong, V. V., Nguyễn, T.-N., & Ziegler, A. D. (2018). Assessing the contribution of porewater discharge in carbon export and CO₂ evasion in a mangrove tidal creek (Can Gio, Vietnam). *Journal of Hydrology*, 563, 303–318. <https://doi.org/10.1016/j.jhydrol.2018.05.042>
- Tait, D. R., Maher, D. T., Macklin, P. A., & Santos, I. R. (2016). Mangrove pore water exchange across a latitudinal gradient. *Geophysical Research Letters*, 43(7), 3334–3341. <https://doi.org/10.1002/2016GL068289>
- Thi Hoa Binh, T., Hoa, P. V., Thoa, L. K., & Luong, N. V. (2008). Using multi-temporal remote sensing data to manage the mangrove for coastal environmental protection. The International Archives of the Photogrammetry, Remote Sensing and Spatial Information Sciences. Vol. XXXVII. Part B8. Beijing 2008.
- Van Loon, A. F., Te Brake, B., Van Huijgevoort, M. H. J., & Dijkema, R. (2016). Hydrological classification, a practical tool for mangrove restoration. *PLoS One*, 11-1, 26. <https://doi.org/10.1371/journal.pone.0150302>
- Wolanski, E., Mazda, Y., & Ridd, P. (1992). Mangrove hydrodynamics. In *Tropical mangrove ecosystems* (pp. 43–62). AGU. <https://doi.org/10.1029/CE041p0043>
- Woodroffe, C. (1992). *Mangrove sediments and geomorphology* (pp. 7–41). AGU. <https://doi.org/10.1029/CE041p0007>
- Xiao, K., Wilson, A. M., Li, H., & Ryan, C. (2019). Crab burrows as preferential flow conduits for groundwater flow and transport in salt marshes: A modeling study. *Advances in Water Resources*, 132, 103408. <https://doi.org/10.1016/j.advwatres.2019.103408>
- Xiao, K., Wilson, A. M., Li, H., Santos, I. R., Tamborski, J., Smith, E., Lang, S. Q., Zheng, C., Luo, X., Lu, M., & Correa, R. E. (2021). Large CO₂ release and tidal flushing in salt marsh crab burrows reduce the potential for blue carbon sequestration. *Limnology and Oceanography*, 66(1), 14–29. <https://doi.org/10.1002/lno.11582>
- Xin, P., Jin, G., Li, L., & Barry, D. A. (2009). Effects of crab burrows on pore water flows in salt marshes. *Advances in Water Resources*, 32(3), 439–449. <https://doi.org/10.1016/j.advwatres.2008.12.008>
- Xiong, Y., Liao, B., Proffitt, E., Guan, W., Sun, Y., Wang, F., & Liu, X. (2018). Soil carbon storage in mangroves is primarily controlled by soil properties: A study at Dongzhai Bay, China. *Science of the Total Environment*, 619–620, 1226–1235. <https://doi.org/10.1016/j.scitotenv.2017.11.187>

SUPPORTING INFORMATION

Additional supporting information may be found in the online version of the article at the publisher's website.

How to cite this article: Arnaud, M., Baird, A. J., Morris, P. J., Taylor, A., Dang, T. H., Tran Hong, H., Dinh Quang, T., Nguyen, T. T., & Polsenaere, P. (2022). The effect of crab burrows on soil-water dynamics in mangroves. *Hydrological Processes*, 36(3), e14522. <https://doi.org/10.1002/hyp.14522>